

Constraints on measurement-based quantum computation in effective cluster states

Daniel Klagges^{1,*} and Kai Phillip Schmidt^{1,†}

¹Lehrstuhl für Theoretische Physik I, Otto-Hahn-Straße 4, TU Dortmund, D-44221 Dortmund, Germany

The aim of this work is to study the physical properties of a one-way quantum computer in an effective low-energy cluster state. We calculate the optimal working conditions as a function of the temperature and of the system parameters. The central result of our work is that any effective cluster state implemented in a perturbative framework is fragile against special kinds of external perturbations. Qualitative aspects of our work are important for any implementation of effective low-energy models containing strong multi-site interactions.

PACS numbers: 03.67.-a, 05.50.+q, 75.10.Jm

A cluster state $|\psi_{\text{CS}}\rangle$ is a quantum state defined on some lattice (we focus on a square lattice) of qubits, which fulfills the following eigenvalue equations

$$K_a := X_a \bigotimes_{b \in \Gamma(a)} Z_b, \quad K_a |\psi_{\text{CS}}\rangle = |\psi_{\text{CS}}\rangle, \quad (1)$$

with X_a and Z_b being Pauli operators acting on qubits a , b , and $\Gamma(a)$ is the set of nearest neighbors of site a . So called one-way quantum computers (1-WQC) perform universal quantum computations just by one-qubit measurements on a cluster state [1]. While this saves the need to apply unitary transformations to the quantum register, it requires to reliably prepare a cluster state. One possibility is to cool the Hamiltonian

$$H_{\text{cl}} := - \sum_{a \in C} K_a \quad (2)$$

into its non-degenerate ground state, which is by definition the cluster state. A direct implementation of H_{cl} is not realistic, as it contains multi-qubit interactions which are not realized in nature.

This suggests to search for a more realistic Hamiltonian with only two-qubit interactions having the same non-degenerate ground state. But such an Hamiltonian does not exist [2], so one is limited to approximate the cluster state. One approach is to use ancillary qubits to effectively mediate the many-qubit interactions. Unfortunately, this is not of practical use, since the necessary precision scales with the system size [3].

Alternatively, one can implement H_{cl} as an effective low-energy model of a realistic Hamiltonian containing only two-qubit interactions [4, 5]. Two questions arise naturally: What are the optimal working conditions to perform measurement-based quantum computation (MBQC) in an effective cluster state? How robust are effective cluster states with respect to external perturbations? In the following, we show that any such effective cluster state, which is implemented in a perturbative framework, is strongly affected by external perturbations.

Model — We replace each qubit on a square lattice by 4 physical qubits and we encode the logical cluster qubit into the subspace defined by the projector

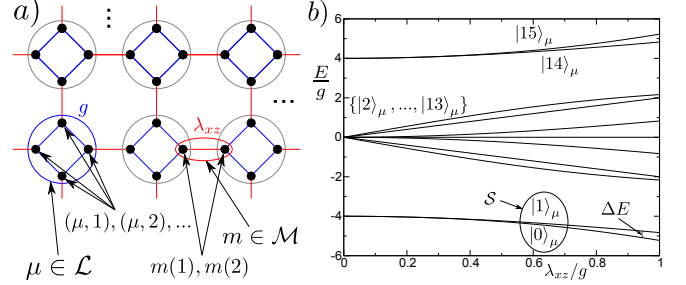


Figure 1. a) Physical qubits (black dots) on a CaVO lattice. The 4 physical qubits of a lattice site $\mu \in \mathcal{L}$ (gray circles) are named with the double indices $(\mu, 1), \dots, (\mu, 4)$. The two physical qubits of a bond $m \in \mathcal{M}$ (red lines) are called $m(1)$ and $m(2)$. To a physical qubit (μ, i) , the neighboring qubit on the bond is $\xi(\mu, i)$. The ZZ -interactions of H_0 are colored blue. b) Energy spectrum of H_μ^{loc} (Eq. 3).

$P := |0_{\text{log}}\rangle \langle 0000| + |1_{\text{log}}\rangle \langle 1111|$ [4]. The Hamiltonian $H := gH_0 + \lambda_{xz}V$ is then defined by:

$$gH_0 := -g \sum_{\mu \in \mathcal{L}} \sum_{i \leftrightarrow j} Z_{(\mu, i)} \otimes Z_{(\mu, j)},$$

$$\lambda_{xz}V := -\lambda_{xz} \sum_{\mu \in \mathcal{L}} \sum_{i=1}^4 X_{(\mu, i)} \otimes Z_{\xi(\mu, i)}.$$

The symbol $i \leftrightarrow j$ means, that the lattice sites i and j are related in some connected graph structure. Other notations are illustrated in Fig. 1a. The ground-state space of H_0 is the space of all logical qubits.

It is possible to solve this model exactly by transforming H into the base Σ^{loc} with the base transformation $CZ_{\mathcal{M}}$ (controlled- Z operators on every bond) [5]. Using $(CZ_{\mathcal{M}}) X_{(\mu, i)} \otimes Z_{\xi(\mu, i)} (CZ_{\mathcal{M}}) = X_{(\mu, i)} \otimes I_{\xi(\mu, i)}$ and $[CZ_{\mathcal{M}}, H_0] = 0$, the transformed Hamiltonian reads $H^{\text{loc}} = \sum_{\mu \in \mathcal{L}} H_\mu^{\text{loc}}$ with

$$H_\mu^{\text{loc}} := -g \sum_{i \leftrightarrow j} Z_{(\mu, i)} \otimes Z_{(\mu, j)} - \lambda_{xz} \sum_{i=1}^4 X_{(\mu, i)} \quad (3)$$

The H_μ^{loc} are local transverse field Ising models (TFIM) on each lattice site μ which can be solved by exact diago-

nalization. If R_μ is the 16×16 matrix of the 16 eigenvectors $|0\rangle_\mu \dots |15\rangle_\mu$ of H_μ^{loc} , the diagonal form of H in the basis Σ^{diag} is: $H^{\text{diag}} := [\bigotimes_{\mu \in \mathcal{L}} R_\mu] H^{\text{loc}} [\bigotimes_{\mu \in \mathcal{L}} R_\mu^\dagger]$ (see Fig. 1b). Most importantly, the gap ΔE between the (unique) ground state $|\psi_H\rangle$ and the first excited state arises perturbatively in order 4 in λ_{xz}/g [5, 6].

It is useful to generalize the cluster stabilizers K_a into the physical space

$$K_\mu := \bigotimes_{i=1}^4 X_{(\mu,i)} \otimes Z_{\xi(\mu,i)} \quad .$$

The K_μ can be also transformed into the basis Σ^{loc} : $K_\mu^{\text{loc}} = (CZ_{\mathcal{M}}) K_\mu (CZ_{\mathcal{M}}) = \bigotimes_{i=1}^4 X_{(\mu,i)}$. In this basis it is easy to show, that the K_μ^{loc} commute with each other and with H^{loc} . Consequently, the eigenvalues ± 1 for each stabilizer K_μ are conserved quantities. For $\lambda_{xz} \rightarrow \infty$, the ground state of H^{loc} is the polarized state which is eigenvector to all K_μ^{loc} with eigenvalue $+1$. The ground state of H in the limit $\lambda_{xz} \rightarrow 0$ is therefore the cluster state of the logical qubits.

The two low-energy states $\{|0\rangle_\mu, |1\rangle_\mu\}$ of H_μ^{loc} represent an effective qubit on the according lattice site μ (see Fig. 1b). We can therefore derive an effective low-energy model in the space \mathcal{S} of all effective qubits

$$H^{\text{diag}}|_{\mathcal{S}} = -\frac{\Delta E}{2} \sum_{\mu \in \mathcal{L}} \tilde{Z}_\mu = -\frac{\Delta E}{2} \sum_{\mu \in \mathcal{L}} K_\mu^{\text{diag}}|_{\mathcal{S}}, \quad (4)$$

where \tilde{Z}_μ being the Pauli Z -operator acting on the effective qubit on the lattice site μ and $K_\mu^{\text{diag}} = R_\mu^\dagger K_\mu^{\text{loc}} R_\mu$. It follows, that the effective low-energy approximation of H in the limit $\lambda_{xz} \rightarrow 0$ is the cluster state Hamiltonian H_{cl} of the logical qubits.

Fidelity — The usability of H for quantum computations depends on the question how “well” the logical cluster state is approximated by $|\psi_H\rangle$. This can be quantified by the fidelity $F = |\langle \psi_H | \psi_{\text{CS}} \rangle|^2$ of two states and its generalization for density operators $F = \langle \psi_{\text{CS}} | \rho | \psi_{\text{CS}} \rangle$ [7]. The fidelity translates to the “success probability” of a MBQC using $|\psi_H\rangle$ as a resource state [5].

As shown in [8], for a Hamiltonian $H_N(\lambda)$ with control parameter λ , size N , and two ground states $\psi_N(\lambda), \psi_N(\lambda')$ it is: $\lim_{N \rightarrow \infty} F(\psi_N(\lambda), \psi_N(\lambda')) = d^N$ with $d \in [0, 1]$ being constant. The “fidelity per site” $d := \lim_{N \rightarrow \infty} \sqrt[N]{F(\psi_N(\lambda), \psi_N(\lambda'))}$ is therefore intensive. Since $d < 1$ for $\lambda_{xz} > 0$, the fidelity of the logical cluster state with $|\psi_H\rangle$ vanishes for $N \rightarrow \infty$. This questions the usability for large systems. However, the concept can still be applied by quantum error correction techniques [5]. In this context the value d translates to the success probability per measurement which must be large enough to fulfill the threshold theorem [9].

We calculate the fidelity $F(|\psi_{\text{CS}}\rangle, \rho) = \langle \psi_{\text{CS}} | \rho | \psi_{\text{CS}} \rangle$ of the logical cluster state $|\psi_{\text{CS}}\rangle$ with the canonical density

operator $\rho := \frac{1}{Z} e^{-\beta H} = \frac{1}{Z} \sum_i e^{-\beta E_{|\psi_i\rangle}} |\psi_i\rangle \langle \psi_i|$. Here $Z = \text{Tr}(e^{-\beta H})$ denotes the partition function, $\beta = \frac{1}{k_B T}$, and one finds

$$F(|\psi_{\text{CS}}\rangle, \rho) = F(|+\rangle_{\mathcal{L}}, \rho_{\mathcal{L}}^{\text{loc}}) = F(|+\rangle_\mu, \rho_\mu^{\text{loc}})^N =: d^N.$$

with $|+\rangle_\mu := 1/\sqrt{2}(|0_{\text{log}}\rangle_\mu + |1_{\text{log}}\rangle_\mu)$. Consequently, it is sufficient to study a single lattice site (we omit index μ)

$$d = \langle + | R^\dagger \rho^{\text{diag}} R | + \rangle = \frac{1}{Z} \sum_{i=0}^{15} e^{-\beta E_{|i\rangle}} |\langle i | R | + \rangle|^2,$$

with $Z = \sum_i e^{-\beta E_{|i\rangle}}$. Next, we approximate $e^{-\beta E_{|i\rangle}} |\langle i | R | + \rangle|^2 \approx 0 \quad \forall i \neq 0$ and $Z \approx e^{-\beta E_{|0\rangle}} + e^{-\beta E_{|1\rangle}}$ which is justified by the following observations:

(a) For MBQC, we have to choose the temperature low enough so that even the first excited state plays a minor role. Due to the exponential scaling factor we can omit all contributions of high-energy states.

(b) Due to the orthogonality of the vectors $|i\rangle$, it is $|\langle i | R | + \rangle|^2 \leq 1 - |\langle 0 | R | + \rangle|^2$ for all $i \in \{1, \dots, 15\}$. For not too large λ_{xz} we expect $|\langle 0 | R | + \rangle|^2 \lesssim 1$, so the contributions of the other states are small.

(c) For the first excited state it is $|\langle 1 | R | + \rangle|^2 = 0$. This is proven by the fact, that $R|+\rangle$ and $|1\rangle$ do not have the same conserved eigenvalue of the K -operator.

The resulting fidelity per site d

$$d \approx \frac{1}{1 + e^{-\beta \Delta E}} |\langle 0 | R | + \rangle|^2. \quad (5)$$

is shown in Fig. 2 for different T . For finite T and for small λ_{xz} , the fidelity is dominated by thermal fluctuations. For large λ_{xz} the curve follows the zero-temperature ground-state fidelity. In between, there is a trade off between both effects. If one assumes an error correction algorithm for a 1-WQC with a simple error model of Pauli errors [10] as it is given in [11] with an error threshold of 1.4% ($d > 0.986$), then the maximum T_{max} where this threshold holds is $T_{\text{max}} = 2.18 \cdot 10^{-4} g/k_B$. It is reached for $\lambda_{xz}^{\text{opt}} = 0.222 g$.

The Hamiltonian H can therefore be used as a 1-WQC under conditions that in principle could be prepared in a laboratory. Next, we determine the robustness of such an effective cluster state against external perturbations.

Z-field — First, we consider the presence of an external field in Z -direction:

$$H_z := gH_0 + \lambda_{xz}V - h_z \sum_{\mu \in \mathcal{L}} \sum_{i=1}^4 Z_{(\mu,i)}.$$

Let us formulate H_z using the basis Σ^{diag} limited to \mathcal{S} . Since the perturbation commutes with $CZ_{\mathcal{M}}$, one has

$$H_z^{\text{diag}}|_{\mathcal{S}} = -\frac{\Delta E}{2} \sum_{\mu \in \mathcal{L}} \tilde{Z}_\mu - 4h_z c(\lambda_{xz}/g) \sum_{\mu \in \mathcal{L}} \tilde{X}_\mu \quad ,$$

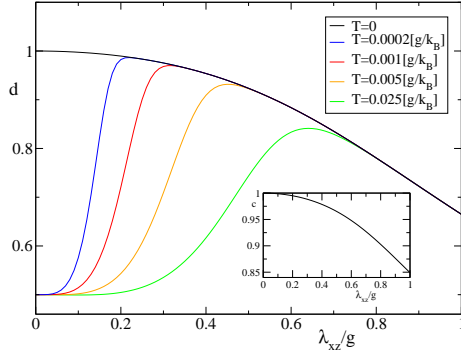


Figure 2. Fidelity per site d (Eq. 5) in dependence of λ_{xz} for different temperatures T . Inset: Contribution $c(\lambda_{xz}/g)$ of a physical Z -operator to the effective \tilde{X} -operator.

where $c(\lambda_{xz}/g) \in \mathbb{R}$ can be read easily from the matrix $R_\mu Z_{(\mu,i)} R_\mu^\dagger$. One finds $\lim_{\lambda_{xz} \rightarrow 0} c = 1$ and the space \mathcal{S} is decoupled from the high-energy space for this limit. The value $c(\lambda_{xz}/g)$ is plotted in Fig. 2. We stress that the scale ΔE is of order 4 in λ_{xz} , while the scale of the \tilde{X} -field is proportional to h_z . One therefore expects a polarization of the ground state for very small ratios h_z/λ_{xz} .

This is confirmed by solving the Hamiltonian H_z exactly in the basis Σ^{loc}

$$H_z^{\text{loc}} = - \sum_{\mu \in \mathcal{L}} \left(H_\mu^{\text{loc}} + h_z \sum_{i=1}^4 Z_{(\mu,i)} \right) =: \sum_{\mu \in \mathcal{L}} H_{z,\mu}^{\text{loc}}$$

which is still a sum of local terms $H_{z,\mu}^{\text{loc}}$. The fidelity per site of the ground state is calculated as in the unperturbed case using the eigenvectors of $H_{z,\mu}^{\text{loc}}$. It can be seen in Fig. 3a that already very small ratios h_z/λ_{xz} have a significant impact on d . For the above example, one finds the upper bound $h_z^{\text{max}} = 1.52 \cdot 10^{-5} g$ satisfying the threshold $d \geq 0.986$ at $T = 0$. Thermal fluctuations play only a minor role, because the gap is strongly increased by the external field [6].

ZZ-coupling — Second, we consider the effect of additional Ising ZZ-couplings on the bonds $m \in \mathcal{M}$

$$H_{zz} := gH_0 + \lambda_{xz}V - \lambda_{zz} \sum_{m \in \mathcal{M}} Z_{m(1)}Z_{m(2)}.$$

Now we formulate the Hamiltonian using the basis Σ^{diag} limited to \mathcal{S}

$$H_{zz}^{\text{diag}}|_{\mathcal{S}} = -\frac{\Delta E}{2} \sum_{\mu \in \mathcal{L}} \tilde{Z}_\mu - \lambda_{zz} c^2(\lambda_{xz}) \sum_{m \in \mathcal{M}} \tilde{X}_{m(1)} \tilde{X}_{m(2)},$$

where again the space \mathcal{S} is decoupled from the high-energy space for the limit $\lambda_{xz} \rightarrow 0$. This Hamiltonian represents a TFIM on the square lattice. For this model a quantum phase transition takes place at $\frac{2\lambda_{zz}|\text{crit}|c^2}{\Delta E} = 0.3285$ separating an ordered from a disordered phase [12]. The gap closes at the critical point

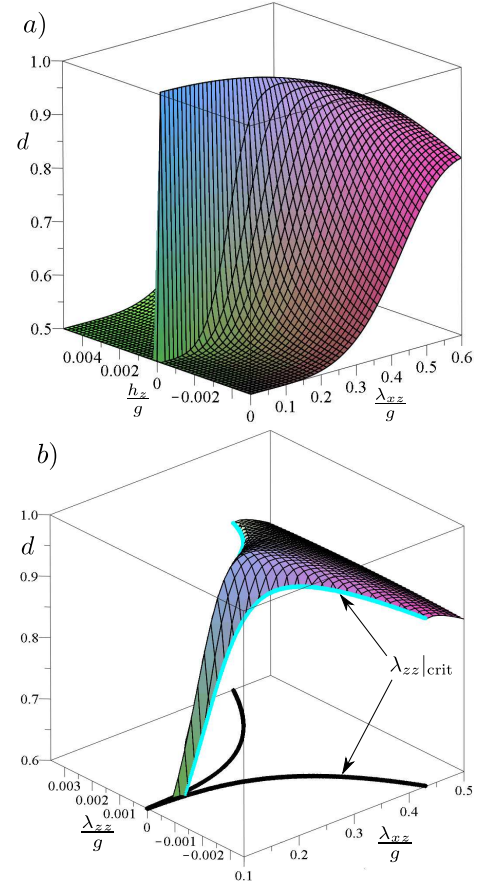


Figure 3. a) Ground-state fidelity per site $d = |\langle 0_z | R_z | + \rangle|^2$ of H_z as a function of λ_{xz} and h_z for $T = 0$. b) Fidelity per site d (Eq. 8) of H_{zz} in dependence of λ_{xz} and λ_{zz} for $T = 0.001 g/k_B$.

changing the ground state significantly, so the system is not useful for MBQC anymore. The energy ΔE is a 4th-order term in λ_{xz} , while the Ising part is of the order λ_{zz} . Very small values $\lambda_{zz}/\lambda_{xz}$ are therefore sufficient to destroy the cluster phase. The estimated critical line $\lambda_{zz}|\text{crit}$ is shown in Fig. 3b as a function of λ_{xz} .

To approximately calculate the fidelity per site for finite temperatures we use the analog of Eq. 5:

$$d \approx \frac{1}{1 + \frac{1}{4\pi^2} \iint_{\vec{k}} e^{-\beta\omega(\vec{k})} d\vec{k}} d(|\psi_{H_{zz}}|_{\mathcal{S}}, |\psi_{\text{CS}}|_{\mathcal{S}}), \quad (6)$$

We note that point (c) is no longer valid as K is no longer conserved, but the use of Eq. 5 is still justified by (a) and (b). The dispersion $\omega(\vec{k}) \approx \sqrt{(\Delta E_{zz})^2 + (v \cdot |\vec{k}|)^2}$ of the first excited mode is taken into account by this equation, while correlated excitations are neglected [13]. The energy gap ΔE_{zz} of the TFIM is calculated by a dlog-Padé [6,6] approximation of its order 13 series expansion [12] and $v = 0.99 \Delta E/2$ [14] is the spin wave velocity at the critical point.

We now transform $|\psi_{\text{CS}}\rangle$ into the effective basis

$$|\psi_{\text{CS}}^{\text{diag}}\rangle_{\mathcal{S}} = \bigotimes_{\mu \in \mathcal{L}} R_{\mu} |+\mu\rangle_{\mathcal{S}} = \bigotimes_{\mu \in \mathcal{L}} |0_{\mu}\rangle \langle 0_{\mu}| R_{\mu} |+\mu\rangle \quad (7)$$

(using $\langle 1|R_{\mu}|+\mu\rangle = 0$) such that Eq. 6 reads

$$d \approx \frac{|\langle 0|R|+\rangle|^2}{1 + \frac{1}{2\pi} \int_0^{2\sqrt{\pi}} e^{-\beta\omega(r)} r dr} d_{\text{TFIM}} \quad (8)$$

where $d_{\text{TFIM}} := d(|\psi_{H_{zz}|\mathcal{S}}\rangle, \bigotimes_{\mu \in \mathcal{L}} |0_{\mu}\rangle)$ corresponds to the ground-state fidelity per site of a TFIM with the polarized state. We have calculated it as a high-order series expansion about the high-field limit

$$d_{\text{TFIM}} = 1 - \frac{1}{8}\lambda^2 - \frac{93}{256}\lambda^4 - \frac{2961}{2048}\lambda^6 - \frac{243005}{32768}\lambda^8 - \frac{812949139}{18874368}\lambda^{10} - \frac{17716040461601}{65229815808}\lambda^{12}$$

where $\lambda := \frac{2\lambda_{zz}c^2}{\Delta E}$ [6].

The fidelity per site of $H_{zz}|_{\text{eff}}$ is plotted in Fig. 3b. One sees, that close to the critical point the fidelity drops due to quantum and thermal fluctuations. For the above example, one finds the upper bound $\lambda_{zz}^{\text{max}} = 8.33 \cdot 10^{-5} g$ satisfying the threshold $d \geq 0.986$ at $T = 0$.

We additionally calculated the energy gap and the ground state fidelity of the full Hamiltonian H_{zz} as series expansions. The high-energy contributions turned out to be negligible corrections to the low-energy results [6].

Conclusions — We have seen that the effective cluster state of H could be used as a 1-WQC under conditions that in principle can be prepared in a laboratory. But to be of practical use, effective cluster states must be also robust against additional perturbations.

We have shown that already very small external perturbations can have a significant impact on effective cluster states. Typically, the effective multi-site interactions yielding the effective cluster state arise in a high order in perturbation theory (here order 4). As a consequence, any external perturbation acting in the effective low-energy model in a lower order (here order 1) represents a strong constraint for the effective implementation of a 1-WQC. This effect is present on any lattice and in any dimension for the problem studied in this work.

The physical mechanism leading to the dramatic loss of fidelity is actually very different for the two perturbations we have considered. The external Z -field leads to a polarization of the ground state and therefore to a reduction of entanglement. The additional Ising coupling induce thermal and quantum fluctuations due to a quantum phase transition.

The qualitative aspects of our work are relevant for a much broader class of problems: any effective low-energy model which is derived perturbatively and which contains dominant multi-site interactions is expected to be affected by external perturbations. The physical reason is

that effective n -site interactions arise typically in order n while it is likely that external perturbations exist which act non-trivially on the effective low-energy degrees of freedom already in a lower order.

A prominent example is Kitaev's honeycomb model which contains the so-called toric code as an effective low-energy model perturbatively in order 4 [15]. The toric code is a topological stabilizer code consisting solely of 4-spin interactions. One can easily show that exactly the same kind of external perturbations studied in this work give again rise to operators in the effective model in order one perturbation theory causing a breakdown of the topological phase for small external perturbations.

In the light of the severe constraints found in this work for the realization of effective cluster states, let us finally mention concepts for MBQC using elementary entities with larger spins which represents a promising route for future research [16–19].

K.P.S. acknowledges ESF and EuroHores for funding through his EURYL.

* klagges@fkt.physik.tu-dortmund.de

† schmidt@fkt.physik.tu-dortmund.de

- [1] R. Raussendorf and H. J. Briegel, *Phys. Rev. Lett.* **86**, 5188 (2001).
- [2] M. A. Nielsen, *Rep. Math. Phys.* **57**, 147 (2006).
- [3] M. Van den Nest, K. Luttmer, W. Dür, and H. J. Briegel, *Phys. Rev. A* **77**, 012301 (2008).
- [4] S. D. Bartlett and T. Rudolph, *Phys. Rev. A* **74**, 040302 (2006).
- [5] T. Griffin and S. D. Bartlett, *Phys. Rev. A* **78**, 062306 (2008).
- [6] See Supplemental Material at [URL will be inserted by publisher] for description of the perturbation methods.
- [7] A. Uhlmann, *Found. Phys.* **41**, 1 (2010).
- [8] H.-Q. Zhou and J. P. Barjaktarevic, *J. Phys. A* **41**, 412001 (2008).
- [9] E. Knill, R. Laflamme, and W. H. Zurek, *Proc. R. Soc. Lond. A* **454**, 365 (1998).
- [10] Strictly this does not cover the two Pauli operator errors of the V -part, but we use it as a reference point.
- [11] R. Raussendorf, J. Harrington, and K. Goyal, *Ann. Phys.* **321**, 2242 (2006).
- [12] H. X. He, C. J. Hamer, and J. Oitmaa, *J. Phys. A* **23**, 1775 (1990).
- [13] M. Troyer, H. Tsunetsugu, and D. Würtz, *Phys. Rev. B* **50**, 13515 (1994).
- [14] C. J. Hamer, *J. of Phys. A* **33**, 6683 (2000).
- [15] A. Kitaev, *Ann. Phys.* **321**, 2 (2006).
- [16] X. Chen, B. Zeng, Z. Gu, B. Yoshida, and I. L. Chuang, *Phys. Rev. Lett.* **102**, 220501 (2008).
- [17] G. K. Brennen and A. Miyake, *Phys. Rev. Lett.* **101**, 010502 (2008).
- [18] J. Cai, A. Miyake, W. Dür, and H. J. Briegel, *Phys. Rev. A* **82**, 052309 (2010).
- [19] T.-C. Wei, R. Raussendorf, and L. C. Kwek, *Phys. Rev. A* **84**, 042333 (2011).

SUPPLEMENTAL MATERIAL

Spectral properties of H

The spectrum of H (and H^{diag}) is the product of the spectra of the local H_μ^{loc} terms. In Tab. I one can see the eigenenergies of the H_μ^{loc} eigenvectors $|0\rangle_\mu, \dots, |15\rangle_\mu$. The unique ground state

$$|\psi_H\rangle = \bigotimes_{\mu \in \mathcal{L}} |0\rangle_\mu$$

of H^{diag} is characterized by all lattice sites being in the $|0\rangle_\mu$ state. The first excited space is N -fold degenerated and is spanned by the states ($\mu \in \mathcal{L}$)

$$|\psi_{\text{EX}}^{(\mu)}\rangle = |1\rangle_\mu \bigotimes_{\nu \in \mathcal{L}/\{\mu\}} |0\rangle_\nu.$$

For the energy gap $\Delta E = E_{|1\rangle_\mu} - E_{|0\rangle_\mu}$ between the ground state and the (N -fold degenerated) first excited space one therefore finds

$$\Delta E = -2g \left(1 + \sqrt{1 + \frac{\lambda_{xz}^2}{g^2}} - \sqrt{2 + 2\frac{\lambda_{xz}^2}{g^2} + 2\sqrt{\frac{\lambda_{xz}^4}{g^4} + 1}} \right).$$

It is independent of the system size. From the Taylor expansion of ΔE one sees, that it is of order 4 in λ_{xz}

$$\Delta E = \frac{5}{8} \left(\frac{\lambda_{xz}}{g} \right)^4 - \frac{7}{32} \left(\frac{\lambda_{xz}}{g} \right)^6 - \frac{21}{512} \left(\frac{\lambda_{xz}}{g} \right)^8 - \frac{33}{2048} \left(\frac{\lambda_{xz}}{g} \right)^{10} + O \left(\left(\frac{\lambda_{xz}}{g} \right)^{12} \right).$$

All of the first N excited spaces can be characterized by some lattice sites being in the $|1\rangle_\mu$ state and all other lattice sites being in the $|0\rangle_\mu$ state. They form the space \mathcal{S} of the effective qubits. The n -th excited space is $\binom{N}{n}$ times degenerated and the gap between the n -th and the $(n+1)$ -th space is ΔE . All high-energy states are characterized by at least one lattice site being in one of the states $|2\rangle, \dots, |15\rangle$. In Fig. 4 you can see the lower part of the spectrum for the example $N = 4$.

State	$E_{ i\rangle_\mu}$
$ 0\rangle_\mu$	$-2g \sqrt{2 + 2\frac{\lambda_{xz}^2}{g^2} + 2\sqrt{\frac{\lambda_{xz}^4}{g^4} + 1}}$
$ 1\rangle_\mu$	$-2g - 2g \sqrt{1 + \frac{\lambda_{xz}^2}{g^2}}$
$ 2\rangle_\mu$	$-2g \sqrt{2 + 2\frac{\lambda_{xz}^2}{g^2} - 2\sqrt{\frac{\lambda_{xz}^4}{g^4} + 1}}$
$ 3\rangle_\mu, 4\rangle_\mu$	$-2g \lambda_{xz}$
$ 5\rangle_\mu$	$2g - 2g \sqrt{1 + \frac{\lambda_{xz}^2}{g^2}}$
$ 6\rangle_\mu, 7\rangle_\mu, 8\rangle_\mu, 9\rangle_\mu$	0
$ 10\rangle_\mu$	$-2g + 2g \sqrt{1 + \frac{\lambda_{xz}^2}{g^2}}$
$ 11\rangle_\mu, 12\rangle_\mu$	$2g \lambda_{xz}$
$ 13\rangle_\mu$	$2g \sqrt{2 + 2\frac{\lambda_{xz}^2}{g^2} - 2\sqrt{\frac{\lambda_{xz}^4}{g^4} + 1}}$
$ 14\rangle_\mu$	$2g + 2g \sqrt{1 + \frac{\lambda_{xz}^2}{g^2}}$
$ 15\rangle_\mu$	$2g \sqrt{2 + 2\frac{\lambda_{xz}^2}{g^2} + 2\sqrt{\frac{\lambda_{xz}^4}{g^4} + 1}}$

Table I. Eigenenergies of the H_μ^{loc} eigenvectors $|0\rangle_\mu, \dots, |15\rangle_\mu$

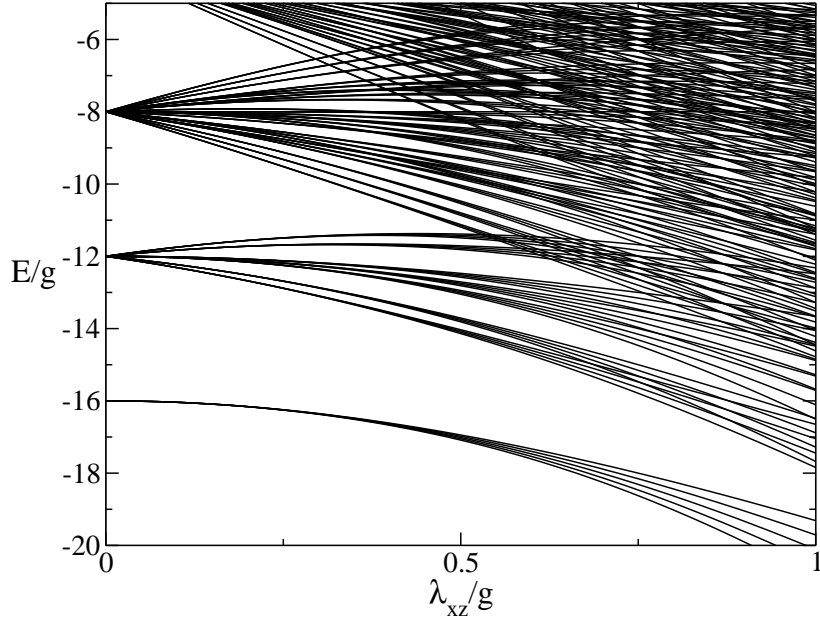


Figure 4. Lower part of the spectrum of H for $N = 4$

Thermal fidelity of H_z

To calculate the fidelity per site for finite temperatures for the case of an external Z -field one must note, that the points (b) and (c) are no longer valid to justify the approximation, since the ground-state fidelity quickly decreases with h_z and since K is no longer a conserved quantity. Because of (a) it still is possible to approximate $e^{-\beta E_{|i_z\rangle}} |\langle i_z | R_z | + \rangle|^2 \approx 0 \quad \forall i \geq 2$ and $Z(\beta) \approx e^{-\beta E_{|0_z\rangle}} + e^{-\beta E_{|1_z\rangle}}$, where R_z is the 16×16 Matrix of the $H_{z,\mu}^{\text{loc}}$ eigenvectors $|0_z\rangle, \dots, |15_z\rangle$. One finds

$$d \approx \frac{1}{1 + e^{-\beta \Delta E_z}} |\langle 0_z | R_z | + \rangle|^2 + \frac{1}{1 + e^{\beta \Delta E_z}} |\langle 1_z | R_z | + \rangle|^2. \quad (9)$$

The energy gap $\Delta E_z = E_{|1_z\rangle} - E_{|0_z\rangle}$, the fidelity $d = |\langle 1_z | R_z | + \rangle|^2$ of the first excited state, and the fidelity per site d for the temperatures $T = 0.0001 g/k_B$ and $T = 0.001 g/k_B$ are shown in Fig. 5. By comparing with the fidelity per site for $T = 0$ (shown in the main paper) one sees, that for finite h_z thermal fluctuations play a minor role, as the gap is increased by the field.

Perturbation method by Takahashi

To calculate the ground-state fidelity per site of the TFIM on a square lattice with the polarized state, the fidelity per site of H_{zz} with the logical cluster state, and the energy gap of H_{zz} as series expansions, we used a perturbation method introduced by Takahashi [1]. In terms of this method a Hamiltonian $H = H_0 + V$ is transferred by a base transformation Γ into an effective Hamiltonian H_{eff} , so that it only acts in one of the H_0 eigenspaces, while the spectral properties are preserved.

Let P be the projector into a H_0 eigenspace L with eigenvalue $E_L^{(0)}$ and \bar{P} be the projector into the according perturbed H eigenspace \bar{L} . The Operator Γ is then defined by

$$\Gamma := \bar{P} P (P \bar{P} P)^{-\frac{1}{2}},$$

with $\Gamma^\dagger \Gamma = P$. The projector \bar{P} can be expressed as

$$\bar{P} = P - \sum_{n=1}^{\infty} \sum_{k_1+k_2+\dots+k_{n+1}=n, k_i \geq 0} S^{k_1} V S^{k_2} V \dots V S^{k_{n+1}} \quad (10)$$

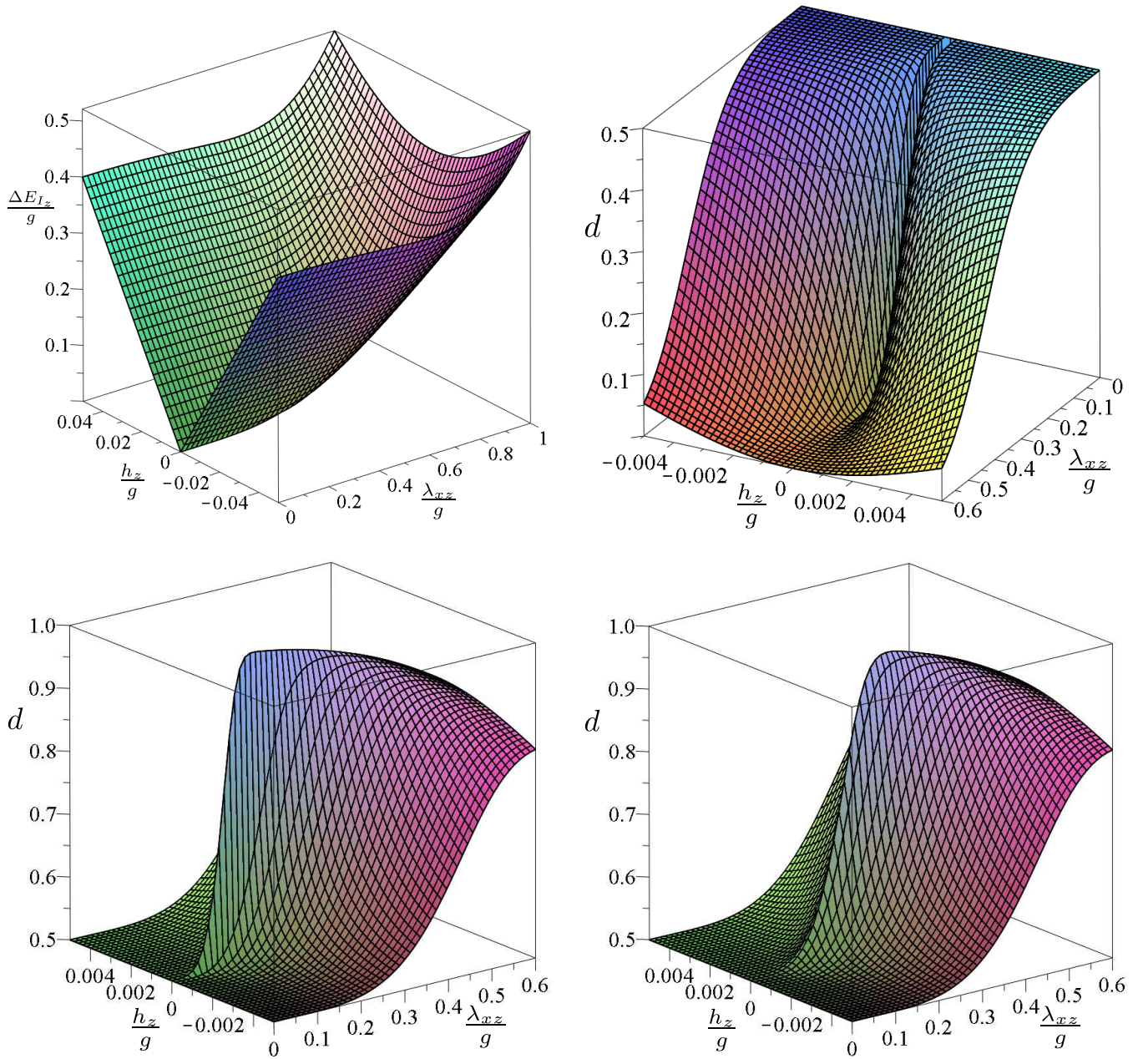


Figure 5. Energy gap $\Delta E_z = E_{|1_z\rangle} - E_{|0_z\rangle}$ (top left), fidelity per site $d = |\langle 1_z | R_z | + \rangle|^2$ of the first excited state (top right), and fidelity per site d (Eq. 9) for the temperatures $T = 0.0001 g/k_B$ and $T = 0.001 g/k_B$ (bottom left and right) for the case H_z of a perturbation with an external Z-field.

with $S^0 := -P$ and $S^k := \left(\frac{1-P}{E_L^{(0)} - H_0} \right)^k$. Together with

$$(P\bar{P}P)^{-\frac{1}{2}} = P + \sum_{n=1}^{\infty} \frac{(2n-1)!!}{(2n)!!} (P(P-\bar{P})P)^n \quad (11)$$

it is now possible to express Γ order by order as a power series of V . Up to order 3 the coefficients of $\Gamma = \sum \Gamma^{(i)}$ are given by

$$\Gamma^{(0)} = P,$$

$$\Gamma^{(1)} = SV P,$$

$$\Gamma^{(2)} = SVSV P - S^2VPVP - \frac{1}{2}PV S^2VP,$$

$$\begin{aligned} \Gamma^{(3)} = & S^3VPVPVP - S^2VSV PVP - SV S^2VPVP \\ & + \frac{1}{2}PV S^3VPVP - S^2VPVSV P + SVSVSV P \\ & - \frac{1}{2}PV S^2VSV P - \frac{1}{2}SV PVS^2VP \\ & - \frac{1}{2}PVSV S^2VP + \frac{1}{2}PVPVS^3VP. \end{aligned}$$

Within the context of this work we calculated the coefficients up to order 13 (7030571 coefficients).

We now transform the Schrödinger equation into the effective basis

$$\begin{aligned} H |\psi_i\rangle &= E_i |\psi_i\rangle \\ \Rightarrow H_{\text{eff}} \Gamma^\dagger |\psi_i\rangle &= E_i \Gamma^\dagger |\psi_i\rangle \end{aligned}$$

with $H_{\text{eff}} := \Gamma^\dagger H \Gamma$. Every eigenvector $|\psi_i\rangle$ of H in \bar{L} therefore corresponds to an eigenvector of H_{eff} in L with the same eigenvalue. It is possible to calculate the perturbed eigenvector $|\psi_i\rangle$ with the base transformation Γ from the according H_{eff} eigenvector $\Gamma^\dagger |\psi_i\rangle$.

To express the effective Hamiltonian $H_{\text{eff}} = \sum H_{\text{eff}}^{(i)}$ as a power series of V we exploit that $[H, \bar{P}] = 0$

$$\begin{aligned} H_{\text{eff}} &= (P\bar{P}P)^{-\frac{1}{2}} P\bar{P}H\bar{P}P(P\bar{P}P)^{-\frac{1}{2}} \\ &= (P\bar{P}P)^{-\frac{1}{2}} P(H_0 + V)\bar{P}P(P\bar{P}P)^{-\frac{1}{2}} \\ &= E_L^{(0)} P + (P\bar{P}P)^{-\frac{1}{2}} PV\bar{P}P(P\bar{P}P)^{-\frac{1}{2}}. \end{aligned}$$

Together with Eqs. 10–11 one finds up to order 4

$$H_{\text{eff}}^{(0)} = E_L^{(0)} P,$$

$$H_{\text{eff}}^{(1)} = PVP,$$

$$H_{\text{eff}}^{(2)} = PVSVP,$$

$$H_{\text{eff}}^{(3)} = PVSVPVP - \frac{1}{2}PVPVS^2VP - \frac{1}{2}PVS^2VPVP,$$

$$\begin{aligned} H_{\text{eff}}^{(4)} = & PVSVPVPVP + \frac{1}{2}PVPVPVS^3VP - \frac{1}{2}PVPVSV S^2VP \\ & - \frac{1}{2}PVPVS^2VSV P - \frac{1}{2}PVSVPVS^2VP - \frac{1}{2}PVSVS^2VPVP \\ & - \frac{1}{2}PVS^2VPVSV P - \frac{1}{2}PVS^2VSV PVP + \frac{1}{2}PVS^3VPVPVP. \end{aligned}$$

Within the context of this work we calculated the coefficients up to order 14 (5394321 coefficients) and for the special case $PVP = 0$ up to order 17 (2490673 coefficients).

Application of Takahashi's method to the energy gap

We applied this perturbation method to calculate the energy gap between the ground state of H_{zz} and its first excited state up to order 5. We start from the representation of H in the basis Σ^{diag} and we define

$$H_0 := H^{\text{diag}},$$

$$V := -\lambda_{zz} \sum_{m \in \mathcal{M}} R_{\mathcal{L}}^\dagger Z_{m(1)} Z_{m(2)} R_{\mathcal{L}}.$$

A method to calculate series expansions for properties of excited states is based on a work by Gelfand [2]. The idea is to interpret excitations on the lattice as quasi-particles and to describe their dynamics. In this quasi-particle picture, the ground state $|\psi_H\rangle$ of H^{diag} corresponds to the vacuum state and the state $|\psi_{\text{EX}}^{(\mu)}\rangle$ corresponds to a state with a single particle at lattice site $\mu = (x, y)$ where (x, y) are Cartesian coordinates. By switching on the perturbation part, dynamics between quasi-particles are induced. Using the effective form H_{eff} of H_{zz} acting solely in the space of the first excited states, we define the hopping elements

$$t_{x,y} := \langle \psi_{\text{EX}}^{(a+x,b+y)} | H_{\text{eff}} | \psi_{\text{EX}}^{(a,b)} \rangle \quad a, b, x, y \in \mathbb{Z}.$$

To this end, it is important that the perturbation V is a sum of local operators each linking two nearest-neighbor lattice sites. A linked process is then defined as a linked operator sequence of these local operators. The linked-cluster theorem [3, 4] states that only linked processes contribute to the one-particle amplitudes. It is therefore possible to retrieve the hopping elements in a given order (in our case order 5) in the thermodynamic limit, although the calculations are limited to finite systems.

To achieve this the finite systems have to be constructed large enough to contain all linked processes of up to 5 bonds. It also follows, that $|x| + |y| > 5 \Rightarrow t_{x,y} = 0$, as there is no order 5 process linking the lattice sites (a, b) and $(a + x, b + y)$ for this case.

The calculation can further be simplified:

1. For symmetry reasons it is

$$t_{x,y} = t_{-x,y} = t_{x,-y} = t_{-x,-y} \quad ,$$

so only one calculation is necessary for such hopping elements.

2. An operator $Z_{m(1)} Z_{m(2)}$ of V anti-commutes with $K_{m(1)}$ and $K_{m(2)}$. It follows that the application of such an operator inverts both K_μ eigenvalues of the two neighboring lattice sites. To contribute to a hopping element, each lattice site must therefore be touched an even number of times by such operators. The only exception to this rule are the lattice sites (a, b) and $(a + x, b + y)$ for $(x, y) \neq (0, 0)$. They must be touched by an uneven number of operators. This allows to further decrease the size of the finite systems. Examples for some hopping elements can be found in Fig. 6.
3. If h is an operator of the power series representation of H_{eff} one can calculate its contribution to a hopping element by calculating $h |\psi_{\text{EX}}^{(a,b)}\rangle$ and multiplying the result with $\langle \psi_{\text{EX}}^{(a+x,b+y)} |$. But to save time and memory it is useful to split the coefficient $h = h_l h_r$ into two parts with roughly the same number of V Operators. The contribution is then calculated by multiplying the two vectors $h_r |\psi_{\text{EX}}^{(a,b)}\rangle$ and $\langle \psi_{\text{EX}}^{(a+x,b+y)} | h_l$.

From the hopping elements we calculate the dispersion of the first excited mode with a Fourier transformation. For the square lattice one finds

$$\omega(k_x, k_y) = t_{0,0} - E_0 + \sum_{(x,y) \neq (0,0)} t_{x,y} \cos(k_x x + k_y y), \quad (12)$$

where E_0 is the ground-state energy of the finite lattice used to calculate $t_{0,0}$. The dispersions for the case $\lambda_{zz} = 0.5g$ and for different λ_{zz} are shown in Fig. 7. The minimal excitation energy (the gap) is at $k_x = k_y = \pi$ for negative λ_{zz} and at $k_x = k_y = 0$ for positive λ_{zz} . The coefficients of the series expansion of the gap up to order 5 are shown in Tab. II for different λ_{zz} . The first-order coefficients equal the coefficient for the TFIM gap. The absolute value of all other coefficients are decreased for finite λ_{zz} . The actual value of the critical $\lambda_{zz}|_{\text{crit}}$ is therefore slightly larger than the critical point calculated using the low-energy approximation (see Fig. 8).

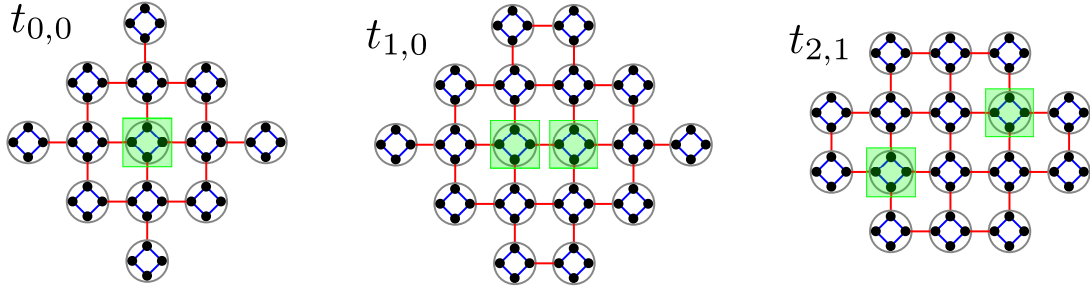


Figure 6. Examples for finite systems to calculate one-particle hopping elements $t_{x,y}$ from the lattice site (a,b) to $(a+x,b+y)$ or vice versa are shown. These two lattice sites are highlighted by a green (gray) background. The finite systems are constructed such that all connected graphs of up to five bonds (a single bond can be counted multiple times) are contained, where each lattice site is touched by an even number of bonds. The only exception to this rule are the lattice sites (a,b) and $(a+x,b+y)$ which must be touched by an odd number of bonds for $(x,y) \neq (0,0)$. The hopping elements of this systems equal the hopping elements of an infinite system up to order 5.

	$c_1 f_1$	$c_2 f_2$	$c_3 f_3$	$c_4 f_4$	$c_5 f_5$
TFIM ($\lambda_{xz} \rightarrow 0$)	-4	-2	-3	-4.5	-11
$\lambda_{xz} = 0.1 g$	-4.000	-2.000	-3.000	-4.500	-11.00
$\lambda_{xz} = 0.2 g$	-4.000	-2.000	-3.000	-4.500	-11.00
$\lambda_{xz} = 0.3 g$	-4.000	-2.000	-3.000	-4.500	-11.00
$\lambda_{xz} = 0.4 g$	-4.000	-2.000	-3.000	-4.500	-11.00
$\lambda_{xz} = 0.5 g$	-4.000	-1.998	-2.998	-4.498	-10.99
$\lambda_{xz} = 0.6 g$	-4.000	-1.992	-2.994	-4.493	-10.97
$\lambda_{xz} = 0.7 g$	-4.000	-1.977	-2.983	-4.480	-10.93
$\lambda_{xz} = 0.8 g$	-4.000	-1.945	-2.959	-4.453	-10.83
$\lambda_{xz} = 0.9 g$	-4.000	-1.888	-2.913	-4.402	-10.64
$\lambda_{xz} = 1.0 g$	-4.000	-1.798	-2.838	-4.319	-10.36

Table II. Coefficients of the energy gap $\Delta E + c_1 \frac{\lambda_{zz}}{g} + c_2 (\frac{\lambda_{zz}}{g})^2 + c_3 (\frac{\lambda_{zz}}{g})^3 + c_4 (\frac{\lambda_{zz}}{g})^4 + c_5 (\frac{\lambda_{zz}}{g})^5$ of H_{zz} up to order 5. The first row shows the coefficients for the TFIM (limit $\lambda_{xz} \rightarrow 0$). It is $f_i := \frac{2}{\Delta E} (\frac{\Delta E}{2g c^2})^i$.

Application of Takahashi's method to the ground-state fidelity

We have applied the perturbation method to calculate the ground-state fidelity per site of H_{zz} with the logical cluster state up to order 4 and the ground-state fidelity per site of a TFIM on a square lattice with the polarized state up to order 12. For H_{zz} , we again use the basis Σ^{diag} and define

$$H_0 := H^{\text{diag}},$$

$$V := -\lambda_{zz} \sum_{m \in \mathcal{M}} R_{\mathcal{L}}^\dagger Z_{m(1)} Z_{m(2)} R_{\mathcal{L}}.$$

For the TFIM, we use

$$H_0 := -\frac{\Delta E}{2} \sum_{\mu \in \mathcal{L}} \tilde{Z}_\mu,$$

$$V := -\lambda_{zz} c^2 \sum_{m \in \mathcal{M}} \tilde{X}_{m(1)} \tilde{X}_{m(2)}.$$

The ground state $|\psi_H\rangle = \bigotimes_{\mu \in \mathcal{L}} |0\rangle_\mu$ of H_0 is in both cases unique and therefore also the only eigenvector of the according H_{eff} . The wave functions of the perturbed ground states can therefore be calculated by applying the base

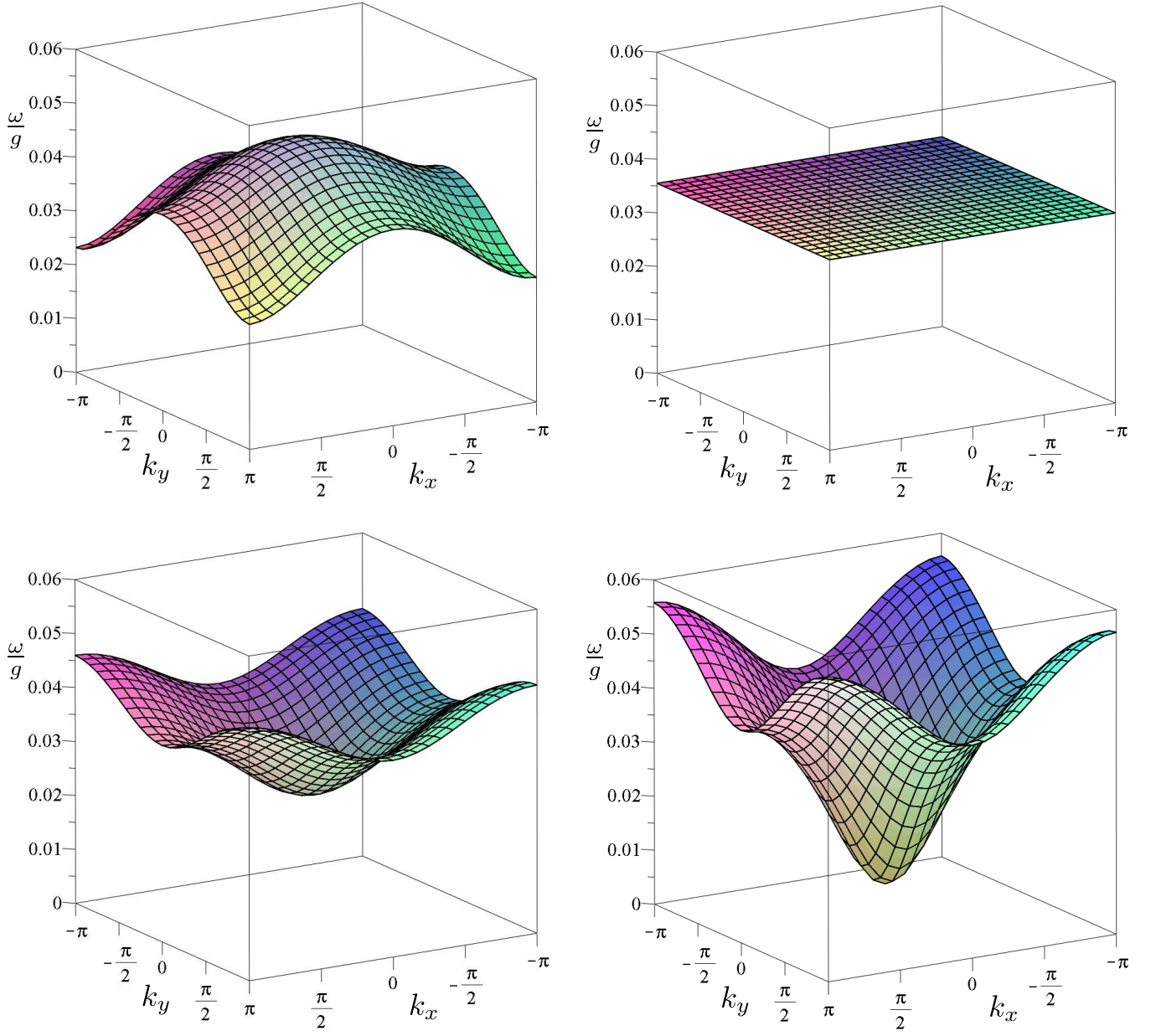


Figure 7. Dispersion of the first excited mode of H_{zz} for $\lambda_{xz} = 0.5g$ up to order 5 for different values of λ_{zz} : $\lambda_{zz} = -0.003g$ (top left), $\lambda_{zz} = 0$ (top right), $\lambda_{zz} = 0.003g$ (bottom left), and $\lambda_{zz} = 0.006g$ (bottom right).

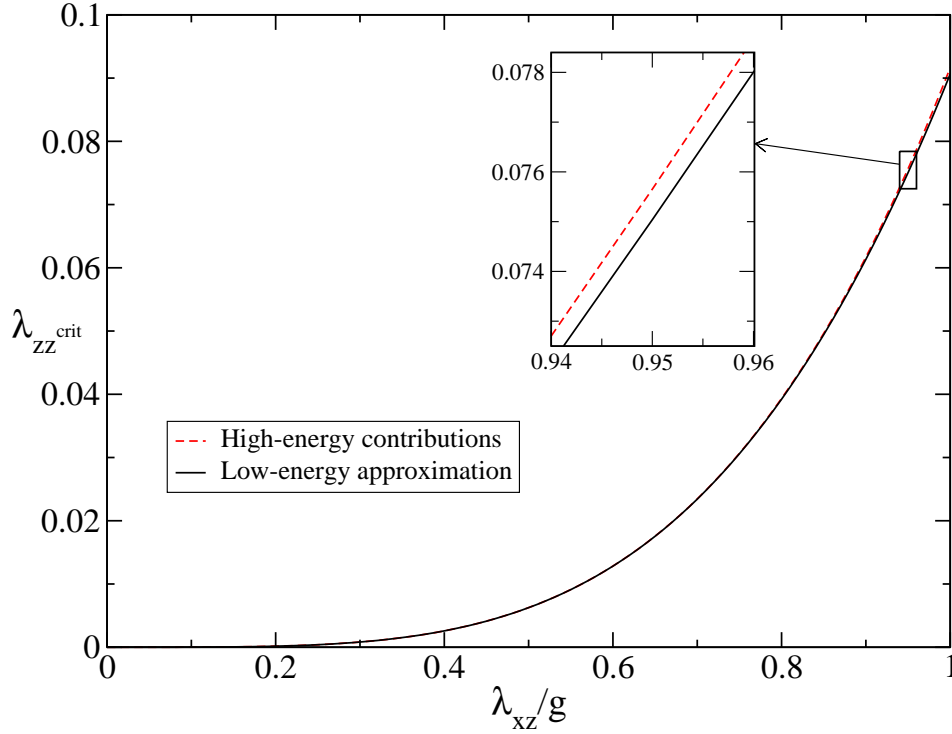


Figure 8. Critical $\lambda_{zz}|_{\text{crit}}$ in dependence of λ_{xz} calculated with the low-energy approximation (black solid line) and corrected by high-energy contributions (red dashed line). The high-energy corrections are calculated by a dlogPadé [2,2] approximation of the order 5 series of the energy gap.

transformation Γ to $\bigotimes_{\mu \in \mathcal{L}} |0\rangle_{\mu}$. For the ground-state fidelity per site one finds

$$d_{H_{zz}}(|\psi_{\text{CS}}\rangle, |\psi_{H_{zz}}\rangle) = \lim_{N \rightarrow \infty} \sqrt[N]{|\langle \psi_{\text{CS}}^{\text{diag}} | \Gamma | 0 \rangle_{\mathcal{L}}|^2},$$

$$d_{\text{TFIM}}(|0\rangle_{\mathcal{L}}, |\psi_{\text{TFIM}}\rangle) = \lim_{N \rightarrow \infty} \sqrt[N]{|\langle 0 |_{\mathcal{L}} \Gamma | 0 \rangle_{\mathcal{L}}|^2}.$$

Again it is possible to exploit the linked-cluster theorem to limit the calculation to finite systems. For example it is sufficient to calculate on a 5×5 lattice with periodic boundary conditions (system lies on a torus) for the order 4 calculation, or a 13×13 lattice for the order 12 calculation respectively.

The calculation can further be simplified.

1. Analog to the second point of the last section only processes can contribute, where each lattice site is touched by an even number of operators located on the bonds. It is easy to see, that this is only possible if the overall number of bonds is even. For the calculations only coefficients of even order must be considered.
2. The 5×5 lattice necessary for the order 4 calculation can be reduced to a 3×5 lattice by bounding it periodically into a “brick wall” structure (see Fig. 9).
3. To reduce the size of the 13×13 lattice for the order 12 calculation another technique was used. The coupling parameter λ_{zz} was replaced by the parameters λ_{\parallel} and λ_{\perp} , so that vertical bonds are associated with λ_{\parallel} and horizontal bonds are associated with λ_{\perp} . Using the rotational symmetry of the lattice the calculation of the order 12 coefficient c_{12} is reduced to the calculation of the λ_{\parallel} and λ_{\perp} coefficients

$$c_{12} \lambda_{zz}^{12} = c_{12}^{(0,12)} (\lambda_{\parallel}^{12} + \lambda_{\perp}^{12}) + c_{12}^{(2,10)} (\lambda_{\parallel}^2 \lambda_{\perp}^{10} + \lambda_{\parallel}^{10} \lambda_{\perp}^2) + c_{12}^{(4,8)} (\lambda_{\parallel}^4 \lambda_{\perp}^8 + \lambda_{\parallel}^8 \lambda_{\perp}^4) + c_{12}^{(6,6)} \lambda_{\parallel}^6 \lambda_{\perp}^6.$$

For the separate calculations of the coefficients $c_{12}^{(0,12)}$, $c_{12}^{(2,10)}$, $c_{12}^{(4,8)}$ and $c_{12}^{(6,6)}$ periodically bounded systems of size 1×13 , 3×11 , 5×9 and 7×7 are sufficient.

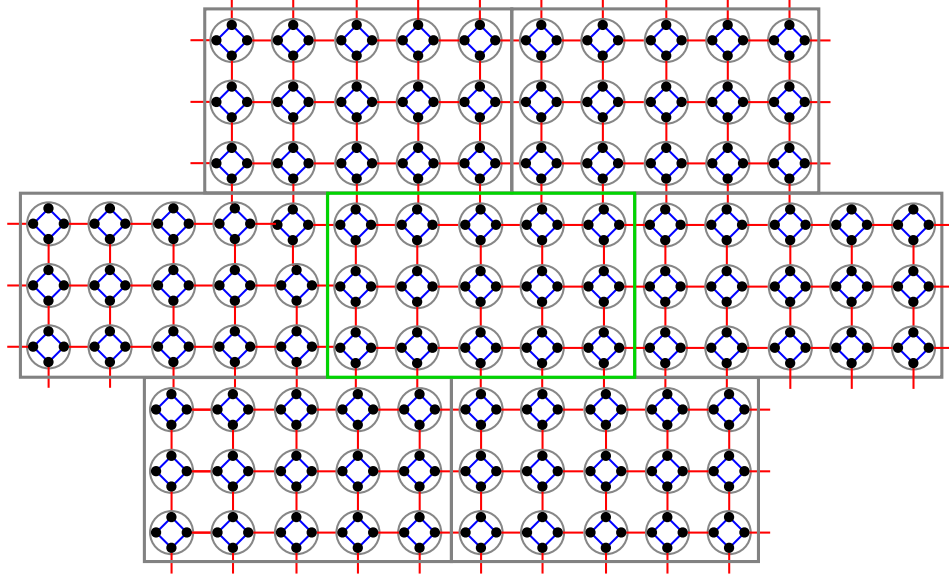


Figure 9. Periodic lattice with “brick wall” boundary conditions. All linked processes of at most 4 bonds cannot form closed loops crossing two opposed lattice boundaries. The order 4 fidelity per site of this lattice is therefore identically to the fidelity in the thermodynamic limit.

4. It is $\langle 0|_{\mathcal{L}} S = 0$. For the calculation of $\langle 0|_{\mathcal{L}} \Gamma |0\rangle_{\mathcal{L}}$ all coefficients with an S -operator at the left side can therefore be left out.
5. Analog to point 3 of the last section it is possible to reduce the calculation of the contribution $\langle 0|_{\mathcal{L}} \gamma |0\rangle_{\mathcal{L}}$ of a coefficient $\gamma = \gamma_l \gamma_r$ of the power series of Γ to the calculation of $\langle 0|_{\mathcal{L}} \gamma_l$ and $\gamma_r |0\rangle_{\mathcal{L}}$ and their product. In principle this can be also applied to the calculation of $\langle \psi_{\text{CS}}^{\text{diag}} | \gamma |0\rangle_{\mathcal{L}}$. Due to the size of the representation of $\langle \psi_{\text{CS}}^{\text{diag}} |$ in the basis Σ^{diag} this does not save time or memory. It is better to calculate $\gamma |0\rangle_{\mathcal{L}}$ and multiply it with $\langle \psi_{\text{CS}}^{\text{diag}} |$ directly.
6. For symmetry reasons the contribution of a process only depends on the shape of the process and not on its position on the lattice. It is therefore possible to limit one of the V -operators (advisably the first) to a single and fixed bond. The resulting value is then the fidelity of the system divided by the number of bonds.

The resulting ground-state fidelity per site of the TFIM on a square lattice with the polarized state is given by

$$d_{\text{TFIM}} = 1 - \frac{1}{8}\lambda^2 - \frac{93}{256}\lambda^4 - \frac{2961}{2048}\lambda^6 - \frac{243005}{32768}\lambda^8 - \frac{812949139}{18874368}\lambda^{10} - \frac{17716040461601}{65229815808}\lambda^{12}.$$

The coefficients of the ground-state fidelity per site of H_{zz} with the logical cluster state are shown in Tab. III. One sees, that the absolute values of the coefficients are decreased for finite λ_{xz} . The actual ground-state fidelity per site of H_{zz} is therefore slightly larger than the fidelity calculated with the low-energy approximation. The fidelity d_{TFIM} and the fidelity of H_{zz} for different λ_{xz} are plotted in Fig. 10.

* klagges@fkt.physik.tu-dortmund.de

† schmidt@fkt.physik.tu-dortmund.de

- [1] M. Takahashi, *J. Phys. C* **10**, 1289 (1977).
- [2] M. P. and Gelfand, *Solid State Commun.* **98**, 11 (1996).
- [3] J. Goldstone, *Proc. R. Soc. Lond. A* **239**, 267 (1957).
- [4] R. F. Bishop, *Theor. Chem. Acc.* **80**, 95 (1991).

	$c_2 \cdot \frac{1}{ \langle 0 R +\rangle ^2} \cdot \left(\frac{\Delta E}{2 \cdot g \cdot c^2}\right)^2$	$c_4 \cdot \frac{1}{ \langle 0 R +L\rangle ^2} \cdot \left(\frac{\Delta E}{2 \cdot g \cdot c^2}\right)^4$
TFIM ($\lambda_{xz} \rightarrow 0$)	-0.125	-0.3633
$\lambda_{xz} = 0.1 g$	-0.1250	-0.3633
$\lambda_{xz} = 0.2 g$	-0.1250	-0.3633
$\lambda_{xz} = 0.3 g$	-0.1250	-0.3633
$\lambda_{xz} = 0.4 g$	-0.1249	-0.3631
$\lambda_{xz} = 0.5 g$	-0.1244	-0.3627
$\lambda_{xz} = 0.6 g$	-0.1232	-0.3612
$\lambda_{xz} = 0.7 g$	-0.1202	-0.3572
$\lambda_{xz} = 0.8 g$	-0.1144	-0.3485
$\lambda_{xz} = 0.9 g$	-0.1051	-0.3321
$\lambda_{xz} = 1.0 g$	-0.09228	-0.3049

Table III. Coefficients of the ground-state fidelity per site $d_{H_{zz}} = |\langle 0|R|+\rangle|^2 + c_2(\frac{\lambda_{zz}}{g})^2 + c_4(\frac{\lambda_{zz}}{g})^4$ of H_{zz} with the logical cluster state for different λ_{xz} . The first row shows the coefficients for the TFIM (limit $\lambda_{xz} \rightarrow 0$).

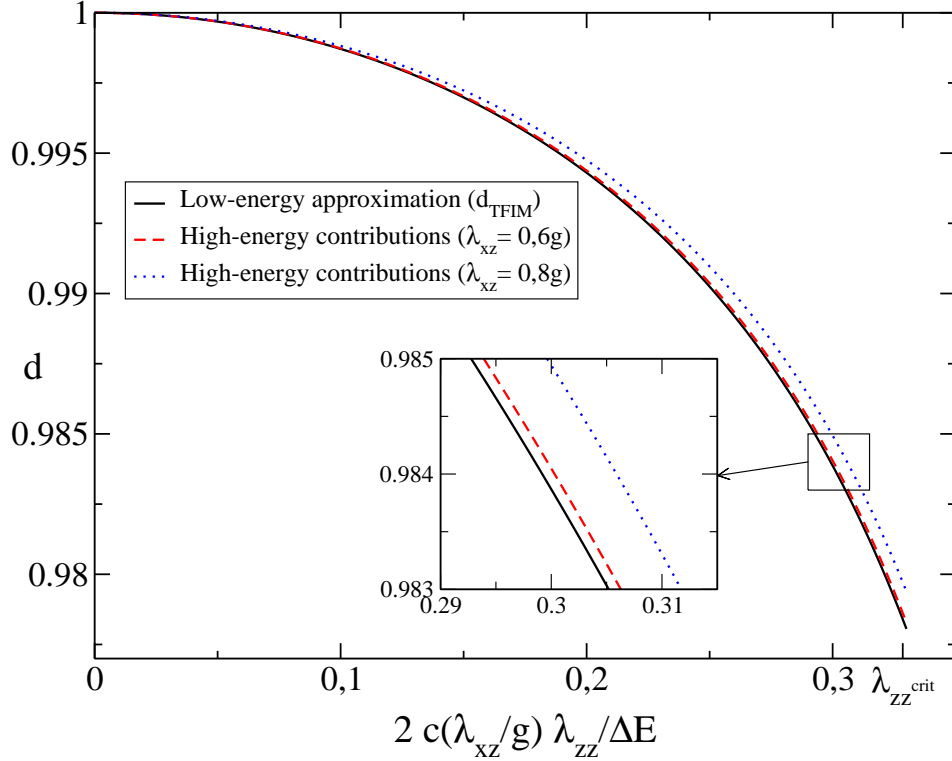


Figure 10. Ground-state fidelity per site d of H_{zz} calculated with the low-energy approximation (d_{TFIM} , shown as solid line) and corrected by high-energy contributions for different λ_{xz} (dashed and dotted lines). The low-energy fidelity is calculated up to order 12 and the corrections are calculated up to order 4.